



Store-Operated Calcium Entry via STIM1 Contributes to MRGPRX2 Induced Mast Cell Functions

Christopher J. Occhiuto^{1†}, Ananth K. Kammala^{1†}, Canchai Yang¹, Rithvik Nellutla¹, Marco Garcia², Gregorio Gomez^{2‡} and Hariharan Subramanian^{1*}

¹ Department of Physiology, Michigan State University, East Lansing, MI, United States, ² Department of Pathology, Microbiology and Immunology, School of Medicine, University of South Carolina, Columbia, SC, United States

OPEN ACCESS

Edited by:

Kottarappat N. Dileepan,
University of Kansas Medical Center,
United States

Reviewed by:

Yosuke Kurashima,
Chiba University, Japan
Toshiaki Kawakami,
La Jolla Institute for Immunology (LJI),
United States

*Correspondence:

Hariharan Subramanian
subram46@msu.edu

[†]These authors have contributed
equally to this work and share first
authorship

‡Present address:

Gregorio Gomez,
Department of Biomedical Sciences,
College of Medicine, University of
Houston, Houston, TX, United States

Specialty section:

This article was submitted to
Inflammation,
a section of the journal
Frontiers in Immunology

Received: 17 August 2019

Accepted: 27 December 2019

Published: 21 January 2020

Citation:

Occhiuto CJ, Kammala AK, Yang C,
Nellutla R, Garcia M, Gomez G and
Subramanian H (2020)
Store-Operated Calcium Entry via
STIM1 Contributes to MRGPRX2
Induced Mast Cell Functions.
Front. Immunol. 10:3143.
doi: 10.3389/fimmu.2019.03143

Mast cells are inflammatory immune cells that play an essential role in mediating allergic reactions in humans. It is well-known that mast cell activation is critically regulated by intracellular calcium ion (Ca²⁺) concentrations. MAS-related G-protein coupled receptor-X2 (MRGPRX2) is a G-protein coupled receptor (GPCR) expressed on mast cells that is activated by various ligands, including several FDA approved drugs; consequently, this receptor has been implicated in causing pseudo-allergic reactions in humans. MRGPRX2 activation leads to an increase in intracellular Ca²⁺ levels; however, the Ca²⁺ mobilizing mechanisms utilized by this receptor are largely unknown. Previous reports showed that store-operated Ca²⁺ entry (SOCE) via the calcium sensor, stromal interaction molecule 1 (STIM1), regulates mast cell response induced by the high-affinity IgE receptor (FcεRI). In this study, using complementary pharmacologic and genetic ablation approaches we demonstrate that SOCE through STIM1 promotes MRGPRX2-induced human mast cell response *in vitro*. Importantly, SOCE also critically modulates MrgprB2 (mouse ortholog of human MRGPRX2) dependent inflammation in *in vivo* mouse models of pseudo-allergy. Collectively, our data suggests that MRGPRX2/MrgprB2 activation of mast cells is dependent on SOCE via STIM1, and further characterization of the MRGPRX2-SOCE-STIM1 pathway will lead to the identification of novel targets for the treatment of pseudo-allergic reactions in humans.

Keywords: mast cells, pseudo-allergic reactions, stromal interaction molecule 1 (STIM1), store-operated calcium entry (SOCE), MAS-related G-protein coupled receptor-X2 (MRGPRX2), MrgprB2

INTRODUCTION

Mast cells are innate immune cells with potent inflammatory properties. They express numerous receptors that respond to mechanical and chemical stimuli; their critical function, however, is eliciting allergic responses through crosslinking of the high-affinity IgE receptor (FcεRI). Following FcεRI ligation, mast cells quickly release histamine from pre-stored vesicles during the acute phase of their response through degranulation, leading to the delayed production and release of inflammatory cytokines (1). The IgE receptor is thus imperative in the development of allergic asthma, rhinitis, and food allergies, all of which result from pathogenic hyperactivity of mast cells (2).

MAS-related G-protein coupled receptor-X2 (MRGPRX2) is a recently identified mast cell receptor known to enhance inflammatory responses independent of FcεRI (3–5). This receptor has been implicated in chronic diseases, such as rosacea (6), urticaria (7), atopic dermatitis (8), and

rheumatoid arthritis (9). MRGPRX2 displays a promiscuous ligand-binding domain that is potently activated by a variety of different cationic peptides and chemical effectors (10–13). The cathelicidin peptide LL-37 (13, 14), neuropeptide cortistatin-14 (CST-14) (10, 15), and mast cell-degranulating molecule compound 48/80 (3, 16) especially, produce robust degranulation responses through MRGPRX2. LL-37 expression is upregulated in patients with chronic inflammatory skin conditions such as rosacea (17), suggesting that mast cell activation via MRGPRX2 may be responsible for the symptoms associated with this disease. In addition, the pathology of several allergic diseases such as asthma (18) and urticaria (7) correlate with mast cell-specific expression of MRGPRX2. Mouse mast cells express MrgprB2, an ortholog of the human receptor (3). This receptor is activated by the same ligands as MRGPRX2 and displays considerable homology with the human receptor. Interestingly, several FDA approved drugs serve as ligands for MRGPRX2 (3, 19–24) and consequently cause pseudo-allergic reactions in humans; however, the mechanism(s) utilized by this receptor to promote mast cell activation is not well-understood.

Mast cell degranulation is preceded by surges of intracellular Ca^{2+} concentrations. Both Fc ϵ RI and MRGPRX2 share similar Ca^{2+} mobilization characteristics (13, 25). Specifically following receptor activation, a rapid increase in intracellular Ca^{2+} is observed that decays very slowly. This sustained Ca^{2+} response induced by MRGPRX2 is surprising, given that MRGPRX2 is a G-protein coupled receptor (GPCR), and most GPCRs induce a transient Ca^{2+} response that almost immediately returns to baseline due to their rapid desensitization and internalization (26). MRGPRX2 displays a prolonged elevation of Ca^{2+} influx comparable to that of the IgE receptor and this response is resistant to desensitization and internalization (13). Mechanistically, Fc ϵ RI uses store-operated Ca^{2+} entry (SOCE), which facilitates endoplasmic reticulum (ER)-induced Ca^{2+} flux and Ca^{2+} signal potentiation (27–29). However, it is currently unclear whether MRGPRX2 utilizes SOCE mechanisms for regulating mast cell responses.

The central proponent of SOCE is an endogenous Ca^{2+} sensor called stromal interaction molecule 1 (STIM1) (30). STIM1 contains ER-lumen oriented Ca^{2+} -binding domains. Upon cell stimulation and depletion of Ca^{2+} in the ER, these domains become unoccupied, causing a conformational shift and extension of arm-like subunits that complex with calcium release-activated calcium (CRAC) channels and transient receptor potential-canonical (TRPC) channels that are expressed on the cell membrane. Subsequent opening of these channels by STIM1 allows for Ca^{2+} influx into the cytosolic space and increased activation of Ca^{2+} -dependent effectors that amplify cellular functions (30, 31).

Since the Ca^{2+} -mobilizing machinery utilized by MRGPRX2 in mast cells is unknown, we sought to characterize the Ca^{2+} signaling responses and the proteins involved in MRGPRX2 Ca^{2+} potentiation. Previous studies have demonstrated that Fc ϵ RI signaling is largely dependent upon SOCE via STIM1 to facilitate proper mast cell function (29, 32–35). Given the potent inflammatory properties of the IgE receptor and MRGPRX2, in conjunction with their analogous Ca^{2+} mobilization responses,

we hypothesized that MRGPRX2 activates SOCE through STIM1. Our data suggests that SOCE via STIM1 is required for MRGPRX2 responses in human mast cells *in vitro*. Additionally, pharmacological inhibition of SOCE attenuated MrgprB2-induced mast cell responses in *in vivo* mouse models of paw edema and rosacea.

MATERIALS AND METHODS

Tissue Culture Media and Reagents

Dulbecco's Modified Eagle's Media (DMEM), penicillin, streptomycin, and L-glutamine supplement were from Corning Cellgro™ (Corning, NY). Recombinant human stem cell factor (hSCF) was purchased from PeproTech (Rocky Hill, NJ). Opti-MEM™ and Stem-Pro™-34 SFM media, puromycin, Lipofectamine® 2000 reagent, and TRIzol™ were purchased from Invitrogen (Carlsbad, CA). Chemical reagents used in buffers, unless otherwise noted, were purchased from Sigma-Aldrich (St. Louis, MO). CST-14 agonist [Pro-c(Cys-Lys-Asn-Phe-Phe-Trp-Lys-Thr-Phe-Ser-Ser-Cys)-Lys], cathelicidin LL-37 (Leu-Leu-Gly-Asp-Phe-Phe-Arg-Lys-Ser-Lys-Glu-Lys-Ile-Gly-Lys-Glu-Phe-Lys-Arg-Ile-Val-Gln-Arg-Ile-Lys-Asp-Phe-Leu-Arg-Asn-Leu-Val-Pro-Arg-Thr-Glu-Ser) and all inhibitors (SKF 96365 HCl (SKF), YM 58483 (YM), A425619, and Nifedipine) were purchased from Tocris Bioscience (Minneapolis, MN). Compound 48/80, substance P and (R)-ZINC-3573 were obtained from Sigma-Aldrich. All kits for cDNA synthesis and quantitative PCR were obtained from Applied Biosystems (Foster City, CA). ELISA kits (TNF- α and IL-2) were purchased from BD Biosciences (Franklin Lakes, NJ). Primary western blotting antibodies (anti-STIM1, anti-phospho-p44/42 (p-ERK1/2) anti-p44/42 (T-ERK1/2), anti-phospho-Akt, anti-Akt, and anti- β -actin) were obtained from Cell Signaling Technology (Danvers, MA) and secondary antibodies (donkey anti-rabbit conjugated to IRDye® 680RD and IRDye® 800CW) were purchased from Li-Cor Biosciences (Lincoln, NE). All shRNA plasmids were purchased from Sigma-Aldrich.

Cells

Human LAD2 cell line was cultured in complete Stem-Pro-34 SFM medium containing penicillin (100 IU/mL), streptomycin (100 μ g/mL) and L-glutamine (2 mM) (PSG) supplemented with recombinant hSCF (100 ng/mL) as described by Kirshenbaum et al. (36). Media was hemi-depleted once every week, and cells were maintained at a concentration of 0.8×10^6 cells/mL. HEK-293T human embryonic kidney cells and rat basophilic leukemia (RBL-2H3) cells were obtained from the American Type Culture Collection (Manassas, VA) and were cultured in DMEM supplemented with 10% bovine calf serum and PSG. Cells were split every other day. RBL-2H3 cells stably expressing MRGPRX2 (RBL-MRGPRX2) were generated as described previously (12, 13) and cells expressing the MRGPRX2 receptor were sorted using flow cytometry and phycoerythrin (PE)-conjugated anti-MRGPRX2 antibody (BioLegend, San Diego, CA). The cells were cultured in the DMEM supplemented with 10% bovine calf serum, PSG and G418 (1 mg/mL).

Human skin mast cells were isolated and cultured as described previously (37, 38). Briefly, mast cells were isolated and purified from fresh surgical specimens of human skin tissues that were purchased from the Cooperative Human Tissue Network (CHTN) of the National Cancer Institute. These studies were approved by the human studies Internal Review Board (IRB) of the University of South Carolina. The tissues were mechanically minced and digested with collagenase type II, hyaluronidase, and DNase I in HBSS buffer (1X HBSS, 0.04% NaHCO₃, 1% fetal bovine serum, 1% HEPES, 0.1% CaCl₂). The samples were filtered through 40 μm cell strainers and separated on a Percoll cushion by density centrifugation. The cells at the interface of buffer and Percoll layers were collected, washed, and resuspended at 5×10^5 cells/mL in serum-free X-VIVO 15™ media (Lonza) supplemented with hSCF (100 ng/mL). They were cultured at 37°C 5% CO₂ with weekly media changes for 8 weeks. Purity was assessed by metachromatic staining with acidic toluidine blue and by flow cytometry staining for FcεRI expression with PE-labeled anti-human FcεRI antibody [clone AER-37 (CRA)] and mouse IgG2bk isotype control (BioLegend). The mast cells were used only when >95% of the cells were FcεRI+ (after ~8 weeks of culture).

Cell Viability Assays

LAD2 cells (0.5×10^5 /well) were plated on 96-well plates and treated with varying concentrations of SKF, YM, Nifedipine, or A425619 for 24 h. The cells were harvested and live and dead cells were counted on a hemocytometer after staining with trypan blue.

Lentiviral Transduction and STIM1 Knockdown

Generation of Lentivirus

Confluent HEK-293T cells (1×10^6 cells) were seeded on to 100 mm² dishes 48 h prior to transfection. Cells were serum-starved for 1 h in Opti-MEM™ medium before addition of Lipofectamine® 2000 reagent and the viral packaging plasmids: p-CMV-VSV-G, pHR8.2ΔR, and STIM1 shRNA (Cat# SHCLNG-NM_003156; TRC# TRCN0000358718) or scrambled-sequence control shRNA (Cat# SCH002). Media was changed to DMEM after 6 h. Seventy-two hours post-transfection, viral supernatant was harvested, 0.4 μm sterile-filtered, and concentrated using Vivaspin™ protein concentrators (100 kDa MWCO, GE Healthcare).

Lentiviral Transduction

LAD2 cells (5×10^6 cells) were washed twice and plated in complete Stem-Pro-34 SFM media supplemented with hSCF (100 ng/mL) and hexadimethrine bromide (polybrene, 4 μg/mL). Concentrated viral supernatant was then added to cells, centrifuged at 700 g for 1 h, and incubated for 8–10 h in 37°C and 5% CO₂. Media was changed and cells were exposed to puromycin (3 μg/mL) for selection of stable clones and viable cells were used for subsequent experiments.

Calcium Mobilization

SOCE Assay

LAD2 cells were washed and resuspended in 1 mL of 0.1% SIR-BSA (118 mM NaCl, 5 mM KCl, 25 mM HEPES, 5.5 mM glucose, 0.4 mM MgCl₂, 1 mM CaCl₂, and 1 mg/mL bovine serum albumin) supplemented with 6 μM Fluo-8 AM calcium dye (Abcam; Cambridge, MA) for 1.5 h at 37°C and 5% CO₂. Cells were then washed twice with Ca²⁺-depleted 0.1% SIR-BSA and 100 μL (0.3×10^6 cells/mL) were seeded in the same buffer with 0.5 mM EGTA. Using the FlexStation® 3 Flex-protocol, changes in fluorescence were measured for 25 min with the addition of CST-14 and reintroduction of Ca²⁺ at indicated time points. Excitation and emission wavelengths were 490 and 520 nm, respectively.

Total Calcium Flux

LAD2 (0.2×10^5 cells in 100 μL) and RBL-2H3 (0.5×10^5 cells in 100 μL) cells were plated in 0.1% SIR-BSA. FLIPR® Calcium 6 dye (Molecular Devices) was reconstituted as per manufacturer's protocol, combined with cells (1:1 ratio) and incubated for 2 h at 37°C and 5% CO₂. Cells were then stimulated with CST-14, LL-37, substance P, compound 48–80, or (R)-Zinc-3573 using the FlexStation® 3 Flex-protocol, and changes in fluorescence were measured over a 120 s period. For assays involving inhibitors, cells were incubated with SKF, YM, Nifedipine, or A425619 for 30 min prior to agonist stimulation. Phosphate-buffered saline (PBS) was used as the control vehicle used for all the inhibitors. Excitation and emission wavelengths were 485 and 525 nm, respectively. Fluorescence data were normalized to maximal response values.

β-Hexosaminidase Release Assay

LAD2 cells were washed twice and resuspended in 0.1% SIR-BSA. Forty-five microliters of cells (0.45×10^6 cells/mL) were seeded and stimulated with CST-14, LL-37, substance P, compound 48–80, or (R)-Zinc-3573 for 25 min. For total β-hexosaminidase release, cells were lysed using 0.1% Triton X-100. The supernatant (20 μL) was collected and incubated with an equivalent volume of 4 mM p-nitrophenyl-N-acetyl-β-D-glucosamine (PNAG) for 1 h at 37°C. The reactions were halted through the addition of 0.1 M NaHCO₃/0.1 M Na₂CO₃ buffer. The β-hexosaminidase release assay for human skin mast cells was performed as described previously by McHale et al. (39). For assays using inhibitors, cells were incubated for 30 min with the appropriate drug prior to agonist stimulations. Inhibitor concentrations were determined using IC₅₀ values reported by the drug manufacturer. Absorbance was measured using FlexStation® 3 multi-mode plate reader (Molecular Devices; San Jose, CA) at 405 nm. Percent of β-hexosaminidase release content was calculated by dividing absorbances of agonist-stimulated cells by total cell β-hexosaminidase content.

ELISA

LAD2 cells (0.25×10^6 cells in 250 μL) were washed twice in cytokine-deprived complete Stem-Pro™-34 media, plated and stimulated with corresponding agonists for 6 h. For experiments involving inhibitors, cells were incubated with the appropriate

drug for 30 min prior to agonist addition. Cells were then centrifuged and the supernatant was collected. Cytokines (TNF- α and IL-2) in the supernatant was determined by ELISA.

Western Blotting

Wild type, STIM1 shRNA or scramble (control) shRNA transduced LAD2 cells (4×10^6 cells) were stimulated for different time intervals with LL-37 (3 μ M) and lysed using radioimmunoprecipitation assay (RIPA) buffer (150 mM NaCl, 1.0% Triton X-100, 0.5% sodium deoxycholate, 0.1% sodium dodecyl sulfate, 25 mM Tris [pH 8.0], and 5 mM EDTA,) with protease inhibitor cocktail (Roche Applied Sciences; Mannheim, Germany). Forty micrograms of protein was loaded in a 10% polyacrylamide gel for electrophoretic separation. Proteins were then transferred to nitrocellulose membranes (GE Healthcare). Membranes were blocked in 5% milk solution for 2 h, washed in Tris-buffered saline [pH 7.6] and 0.1% Tween-20 (TBST), then probed with primary antibodies (anti-STIM1, anti-phospho-p44/42, anti-p44/42, anti-phospho-Akt, anti-Akt, and anti- β -actin). The following day, blots were washed in TBST and probed with LiCor IRDye[®] 680RD or IRDye[®] 800CW conjugated secondary antibodies for 2 h in the dark. Blots were imaged using LI-COR Odyssey Imaging Systems and analyzed using Image Studio[™] Lite (LI-COR Biosciences).

Mice

C57BL/6 and Balb/c mice were obtained from the Jackson Laboratory (Bar Harbor, ME). All mice were kept under specific pathogen-free conditions. All experiments had the approval of the Institutional Animal Care and Use Committee at Michigan State University. Both male and female mice (6–8 weeks old) were used for experiments.

Paw Edema Model

C57BL/6 mice were initially treated with PBS (vehicle) or the SOCE inhibitor SKF (30 mg/kg) for 2 days via i.p. injection (3, 22, 40). On the 3rd day, mice received PBS in the right hind paw and compound 48/80 (150 ng in 5 μ L) in the left hind paw along with SKF (i.p.). Mice were then injected with 0.15% Evans blue i.v. After 30 min, the thickness of the paws was measured using a micrometer thickness gauge (Peacock thickness gauge, G-1A). The paws were excised, weighed, dried at 50°C, and placed in 1 mL acetone:saline (7:3) for 48 h. The absorbance of the supernatant (250 μ L) was quantified at 650 nm.

Serum Histamine Analysis by LC-MS/MS Method

To estimate the serum histamine levels, we used the method developed by Chimalakonda et al. (41), with a few modifications. After 30 min of compound 48/80 injection in the paws, mice were culled and blood was collected. The serum samples were mixed with three volumes of acetonitrile, vortexed, and centrifuged at $3,000 \times g$ at 4°C for 10 min. The supernatant was dried

in a vacuum evaporator and reconstituted in mobile phase (10 mM perfluoroheptanoic acid (PFHA) in water) for LCMS/MS analysis. Histamine standards and spiked serum samples were prepared in mobile phase.

LCMS analysis was performed using a Waters Quattro Micro interfaced with an H-class Waters Acquity UPLC. A Supelco Ascentis Express C18 HPLC column (2.1 \times 100 mm, 2.7 μ m particle size) was maintained at 40°C in a column oven. The following UPLC-ESI-MS/MS system conditions were used: a mobile phase of solvent A (10 mM PFHA in water) and solvent B (acetonitrile) with gradient elution of solvent B at 10% at time 0 min then ramped to 99% B at 3.50 min, hold at 99% B from 3.50 to 4.50 min and return to 10% acetonitrile at 4.51 min until 6 min with a 0.3 mL min⁻¹ flow rate. MS settings were as follows: electrospray ionization in positive ion mode; capillary voltage 2 kV; source temperature 120°C; desolvation temp 350°C; desolvation gas flow 800 L/h. Histamine was monitored using an MRM method with an m/z 112 to 95 transition. Cone voltage was 22 V and collision energy was 16 V with a dwell time of 0.2 s.

Experimental Rosacea Model

Balb/c mice received i.p. injections of PBS (vehicle) or SKF (30 mg/kg) for 2 days. Mice were then given intradermal injections of LL-37 (50 μ L of 320 μ M) in their dorsal skin twice a day for 2 days (6) while continuing the SKF treatment. Seventy-two hours after the last LL-37 injection, skin tissues were harvested and either snap-frozen in liquid N₂ for RNA analysis or fixed in 10% formalin solution for H&E staining. For some experiments, mice were injected with a single dose of LL-37 (50 μ L of 320 μ M) after the SKF treatments and the skin tissues were harvested and fixed in 10% formalin solution 30 min after the LL-37 injection. Skin inflammation was scored as described previously by Schwartz et al. (42). Briefly, an objective scoring system was employed in a blinded fashion. Erythema, scaling and thickening were scored independently from 0 to 4 as follows: 0, none; 1, slight; 2, moderate; 3, marked; 4, extreme. The average cumulative score of erythema, scaling and thickening served to indicate the inflammation score (scale 0–4). For epidermal thickness measurements, five random epidermal areas in H&E stained skin sections from each mouse were chosen and measured following the acquisition of images using a Nikon[®] ECLIPSE 50i microscope equipped with a Lumenera[®] Infinity 3 color camera. For assessing *in vivo* mast cell degranulation, skin tissues were stained with toluidine blue (0.1% in PBS, pH 2.3) and images were captured as described above. Degranulated mast cells (as determined by the staining intensity, appearance, and/or location of the granules) were counted and expressed as percentage of total mast cells in the tissue sections (43).

Real-Time PCR

Skin samples taken from mice were homogenized in liquid N₂ using a mortar and pestle. RNA was extracted using TRIzol[™] reagent according to the manufacturer's protocol. RNA (2 μ g)

was transcribed to cDNA using the high capacity cDNA reverse transcription kit from Applied Biosystems. RNA levels (*Ccl2*, *Il6*, *Tnf*, *Mmp9*, *Tpsab1*, and *Cma1*) were quantified using gene expression assays with TaqMan™ Fast Advanced Master Mix and validated TaqMan™ probes.

Statistics

Statistical analyses were performed using GraphPad PRISM software (San Diego, CA). A *p*-value less than or equal to 0.05 was deemed to be significant.

RESULTS

SOCE Inhibitors Attenuate MRGPRX2 Mediated Ca^{2+} Mobilization, Degranulation, and Cytokine Production in Human Mast Cells

To determine the mechanisms via which MRGPRX2 activation induce Ca^{2+} influx, we activated LAD2 human mast cells with the known MRGPRX2 agonist CST-14 (10) in the presence of drugs that target Ca^{2+} channels and/or Ca^{2+} -mobilizing

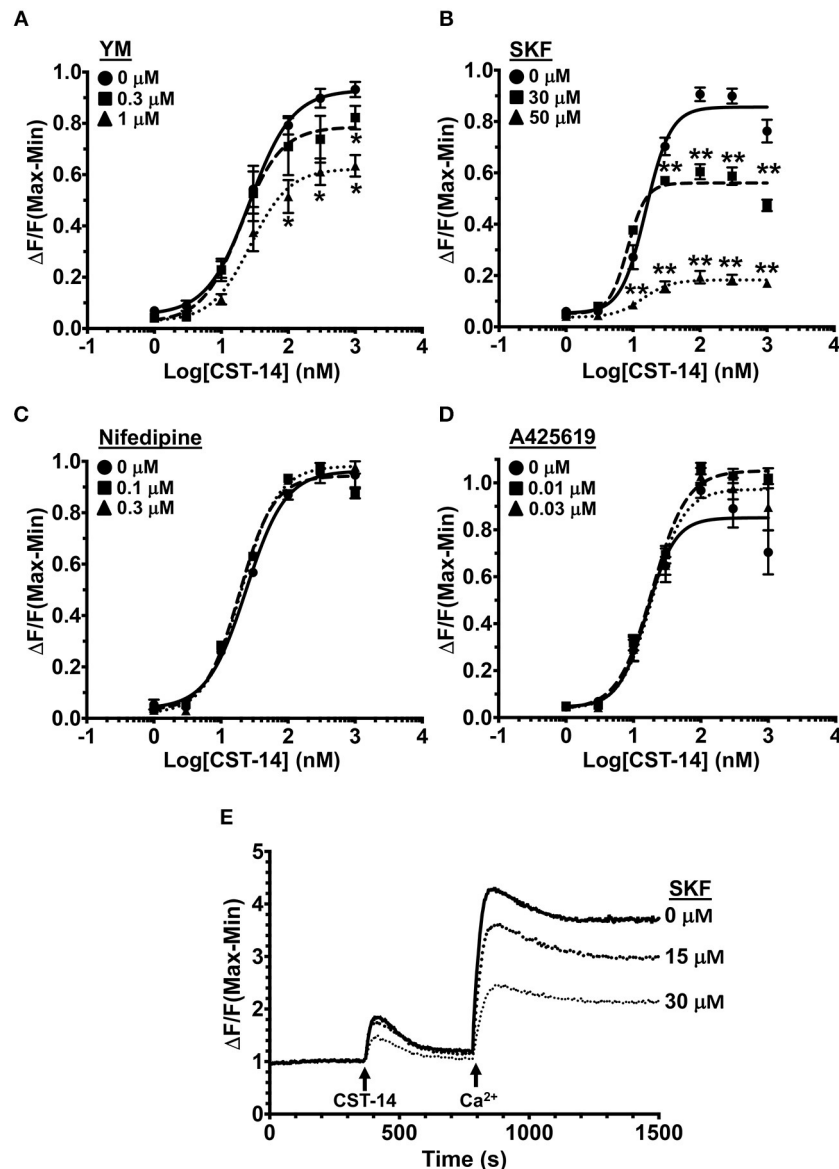


FIGURE 1 | MRGPRX2-induced Ca^{2+} mobilization is reduced by SOCE inhibition. (A–D) Intracellular Ca^{2+} mobilization in LAD2 human mast cells was determined following incubation with varying concentrations of (A) YM, (B) SKF, (C) Nifedipine, and (D) A425619 for 30 min. Cells were treated with half log doses of the MRGPRX2 agonist cortistatin-14 (CST-14), and changes in fluorescence intensities were recorded for 120 s. Data are plotted as the change in fluorescence [minimum (Min) subtracted from maximum (Max) value] normalized to the maximal change in fluorescence. (E) Traces show SOCE assay following SKF pretreatment. LAD2 cells were suspended in Ca^{2+} -free buffer and stimulated with 300 nM CST-14. CaCl_2 (Ca^{2+}) at a final concentration of 2 mM was added to the cells at the indicated timepoint. Plotted curves are the average (mean \pm S.E.) of 3–6 independent experiments. Data are analyzed with two-way ANOVA. **p* < 0.05 and ***p* < 0.01.

proteins. The doses of the inhibitors were chosen based on the previously reported IC₅₀ values (concentration at which 50% inhibition is observed). The inhibitors did not display any mast cell cytotoxicity at the concentrations used for experiments (Figure S1). Exposure to YM 58483 (YM, IC₅₀ is 0.3–1 μM), an antagonist for calcium release-activated calcium (CRAC) channels (such as ORAI1), significantly decreased the

mobilization of intracellular Ca²⁺ (Figure 1A). ORAI channels are activated by the ER Ca²⁺ sensor STIM1 (44, 45). To determine if SOCE via STIM1 contributes to MRGPRX2-induced Ca²⁺ response, we exposed cells to a SOCE inhibitor SKF 96365 HCl (SKF, IC₅₀ is 10–50 μM). A significant dose-dependent reduction in Ca²⁺ influx was observed with SKF suggesting that MRGPRX2-induced Ca²⁺ mobilization is regulated by SOCE

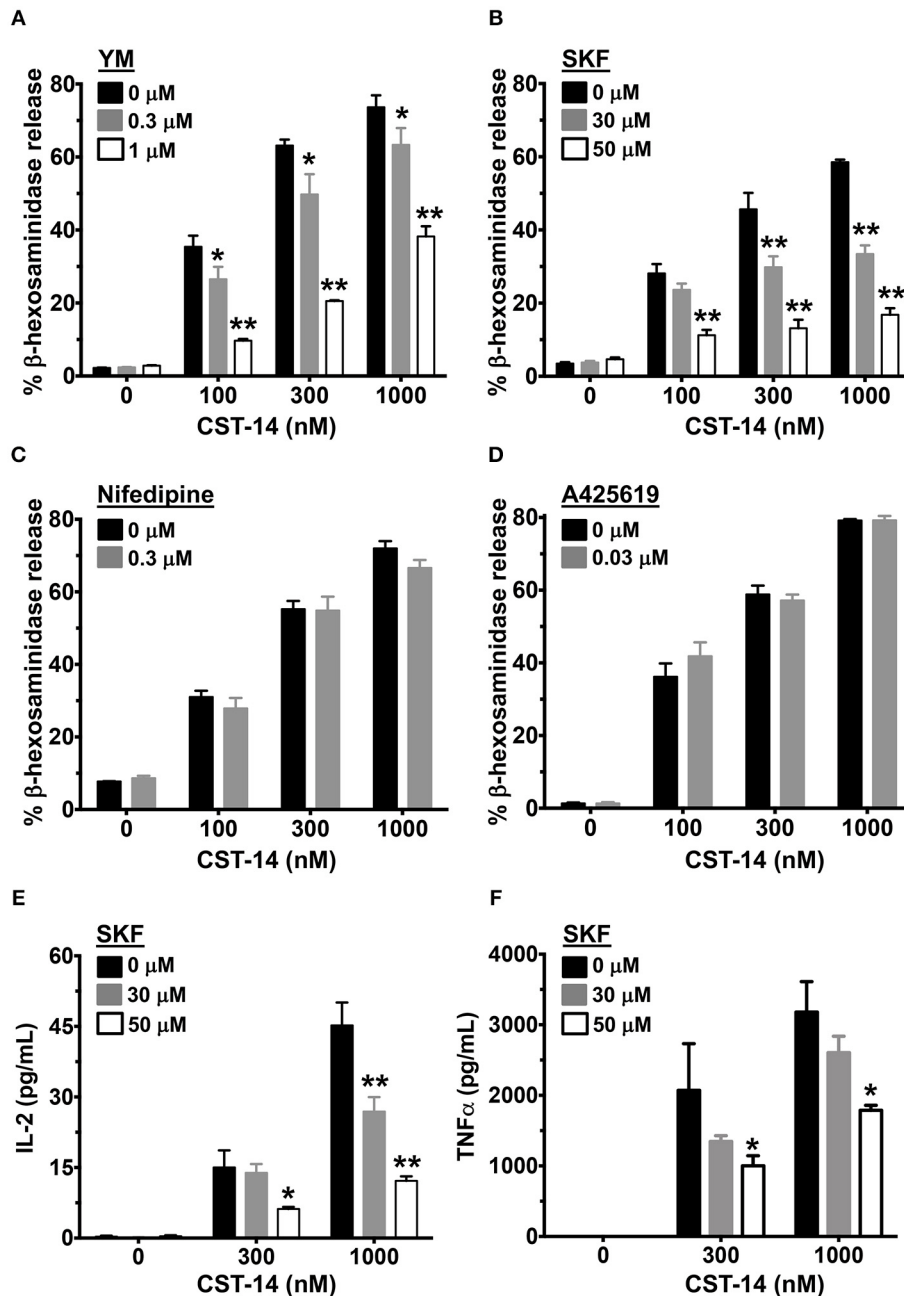


FIGURE 2 | Mast cell degranulation and cytokine production are inhibited by SOCE antagonists. (A–D) CST-14-induced degranulation in LAD2 mast cells as quantified by β-hexosaminidase release in the presence of (A) YM, (B) SKF, (C) Nifedipine, and (D) A425619 is shown. Values are plotted as percentages of total cell lysate β-hexosaminidase content. (E,F) Bar graphs show IL-2 and TNF-α production by LAD2 mast cells stimulated with the indicated concentrations of CST-14. Data shown are mean ± S.E. of 3–5 independent experiments. Statistical significance was determined by two-way ANOVA. **p* < 0.05 and ***p* < 0.01.

via STIM1 and ORAI (Figure 1B). Given the potential off-target effects that SKF may have, we examined the role of voltage-gated Ca^{2+} channels and TRP channels that are known to be susceptible to SKF treatment (46, 47). Nifedipine, an L-type channel antagonist, and A425619, a TRP channel antagonist, did not affect MRGPRX2-induced Ca^{2+} influx (Figures 1C, D) suggesting that SKF indeed targets SOCE via STIM1. Finally, to conclusively verify the role of SOCE, LAD2 cells were placed into Ca^{2+} -free buffer and stimulated with CST-14 (Figure 1E). The cells displayed a small, transient increase in fluorescence followed by a rapid return to baseline. Upon re-addition of Ca^{2+} to the buffer, a surge of Ca^{2+} -flux into the cell was observed, though SKF diminished this response in a dose-dependent fashion.

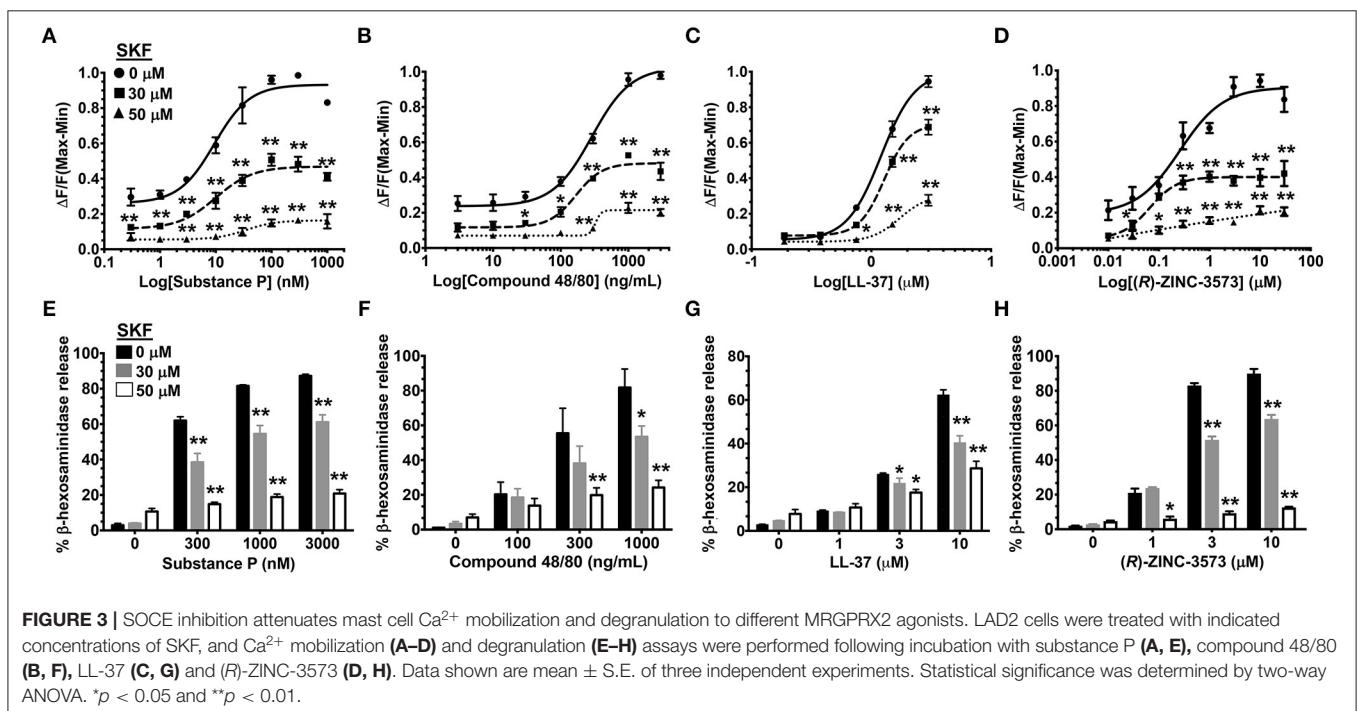
Since Ca^{2+} is an important second messenger that regulates the functional responses of mast cells such as degranulation and cytokine production, we analyzed the effects of SOCE inhibition on these mast cell functions. The degranulation response of LAD2 cells (as assessed by the release of β -hexosaminidase) to CST-14 was significantly reduced following pre-treatment with YM and SKF (Figures 2A,B). Consistent with our data in the Ca^{2+} mobilization assays (Figures 1C,D), the L-type Ca^{2+} and TRP channel inhibitors (Nifedipine and A425619) did not have any effect on CST-14-induced mast cell degranulation (Figures 2C,D). These data thus support the role for SOCE via STIM1 and the CRAC channels as the predominant mechanism of Ca^{2+} entry and subsequent mast cell degranulation. Next, we assessed if SOCE regulates delayed mast cell response such as cytokine production following MRGPRX2 stimulation. SKF treatment significantly inhibited the production of IL-2 (Figure 2E) and TNF- α (Figure 2F) in a

dose-dependent fashion. Collectively, our data demonstrates that the release of inflammatory mediators by mast cells following MRGPRX2 stimulation is dependent upon Ca^{2+} mobilization through SOCE.

SKF Inhibits Ca^{2+} Mobilization and Degranulation Induced by Different MRGPRX2 Ligands

MRGPRX2 is a GPCR that is activated by several ligands that share amphipathic properties (11, 13, 15, 16). As such, the neuropeptide substance P, compound 48/80, and the cathelicidin LL-37 induce potent Ca^{2+} mobilization and mast cell degranulation via MRGPRX2 (3, 13, 16). A recent study (48) identified a synthetic ligand [(R)-ZINC-3573] as a potent selective agonist for MRGPRX2. To determine if SOCE is required for MRGPRX2 response induced by these ligands, we exposed LAD2 mast cells to different concentrations of the agonists in the presence of SKF and assessed for Ca^{2+} mobilization and degranulation response. Our data demonstrates that both Ca^{2+} mobilization (Figures 3A–D) and degranulation (Figures 3E–H) in response to substance P, compound 48/80, LL-37 and (R)-ZINC-3573 are substantially reduced in the presence of SKF.

RBL-2H3 is a rat basophilic cell line that has been used extensively to assess mast cell activation (49–54). These cells do not endogenously express MRGPRX2 and hence do not respond to CST-14 (16). To determine the specificity of SKF in attenuating MRGPRX2 activation, we generated RBL-2H3 cells stably expressing MRGPRX2 (RBL-MRGPRX2) and sorted cells expressing high levels of this



receptor by flow cytometry (Figure S2A). In agreement with previous reports (13, 16, 55), wild type RBL-2H3 (RBL-2H3 WT) cells did not respond to the MRGPRX2 agonists, compound 48/80, substance P, LL-37, and CST-14 for Ca^{2+} mobilization (Figure S2B). However, stable expression of MRGPRX2 rendered these cells responsive to MRGPRX2 stimulation. Consistent with our observation with LAD2 cells, intracellular Ca^{2+} mobilization in RBL-MRGPRX2 cells following stimulation with compound 48/80, substance P, LL-37, and CST-14 was significantly inhibited by SKF (Figure S2B).

SKF Treatment Affects Mitogen-Activated Protein (MAP) Kinase Activation Following MRGPRX2 Stimulation of Mast Cells

MRGPRX2 activation results in downstream signaling events that activate the MAP kinase and Akt pathways that ultimately regulate mast cell responses such as degranulation and cytokine production (56, 57). Since SOCE regulated mast cell degranulation and cytokine production following MRGPRX2 activation (Figures 2, 3), we examined whether the upstream signaling events were also regulated via the same mechanism. We exposed LAD2 cells to LL-37 for different time intervals,

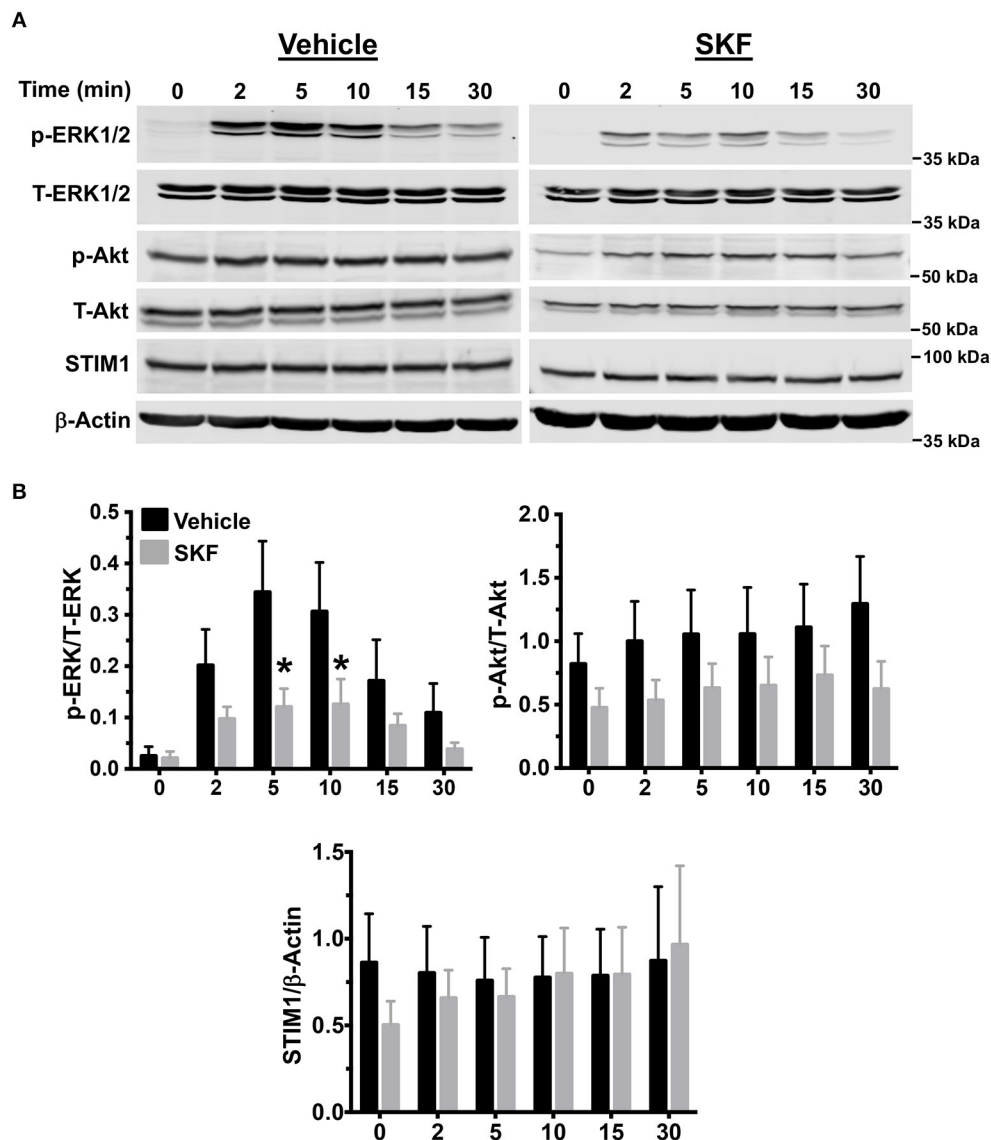


FIGURE 4 | MAP kinase signaling following MRGPRX2 activation is inhibited by SOCE reduction. LAD2 cells were treated with vehicle (PBS) or SKF (30 μ M) and exposed to LL-37 (3 μ M) for different time intervals. **(A)** Representative western blots are shown. The blots with phosphorylated proteins (p-ERK1/2 and p-Akt) were stripped and reprobbed with the total protein (T-ERK1/2 and T-Akt) antibodies. The STIM1 blot was stripped and reprobbed with β -Actin (loading control). **(B)** Bar graphs show relative intensities of bands for the indicated signaling proteins. Phosphoproteins were normalized to total expression for each respective target. STIM1 was normalized to β -Actin levels. Data from three independent experiments are shown. Statistical significance was determined by Student's *t*-test. **p* < 0.05.

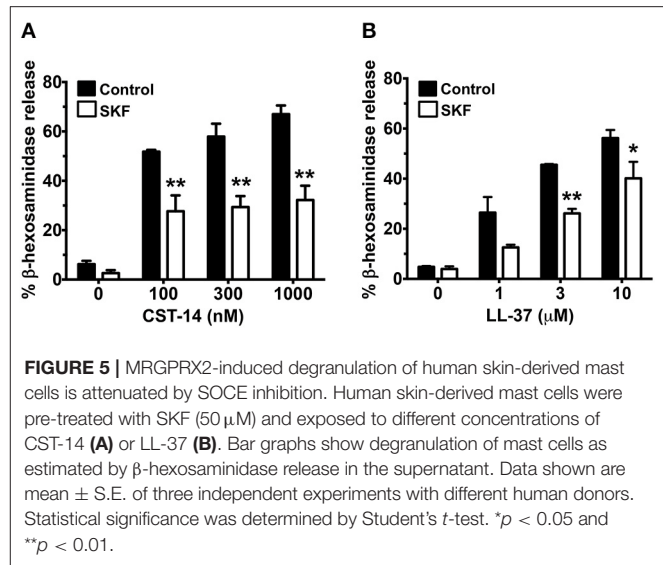
either in the presence or absence of SKF and analyzed for MAP kinase and Akt activation by Western blotting. Transient phosphorylation of the MAP kinase ERK1/2 was evident following LL-37 stimulation, with levels returning to baseline by 30 min. Notably, ERK1/2 phosphorylation was significantly inhibited by treatment with SKF at the 5- and 10-min time points (Figures 4A,B). Contrary to this result, Akt phosphorylation was not altered in the presence of SKF, suggesting that SOCE regulates the MAP kinase but not the Akt pathway following MRGPRX2 stimulation. Additionally, there were no changes in STIM1 expression levels after SKF treatment, indicating that the altered mast cell Ca^{2+} mobilization and functional responses were not due to reduced STIM1 expression following SKF treatment. Taken together, our data suggests that SOCE inhibition following MRGPRX2 activation attenuates Ca^{2+} mobilization and downstream MAP kinase signaling events; thus, diminishing functional responses such as degranulation and cytokine production.

SKF Inhibits MRGPRX2 Mediated Degranulation of Primary Skin-Derived Human Mast Cells

Previous reports have shown that primary human mast cells derived from the peripheral blood as well as human skin mast cells express MRGPRX2 and respond to MRGPRX2 agonists (6, 7, 13). To confirm the biological relevance of our studies obtained with LAD2 cells, we cultured mast cells isolated from the human skin and then exposed these cells to SKF and assessed their degranulation response to different concentrations of CST-14 and LL-37. Consistent with our data from LAD2 cells, SKF treatment significantly reduced degranulation of human skin mast cells to these MRGPRX2 agonists (Figures 5A,B).

Knockdown of STIM1 Ablates MRGPRX2-Induced Mast Cell Response

Pharmacological targeting, in most cases, is prone to off-target effects. To confirm the accuracy of our results obtained with the SKF treatment, we conducted additional experiments where we specifically deleted STIM1 expression in LAD2 mast cells using lentiviral shRNA transduction (12, 13) and performed functional assays with these cells. We used scrambled shRNA transduced cells as controls for our experiments. STIM1 expression levels were reduced (by ~80%) as determined by western blotting (Figure 6A). As expected, SOCE was substantially reduced in STIM1 knockdown cells (Figure 6B). Consistent with the results obtained with SKF and YM (Figures 1–3), degranulation responses to CST-14 (Figure 6C) and LL-37 (Figure 6D) were significantly reduced in cells transduced with STIM1 shRNA, as compared to scramble (control) shRNA-transduced cells. Furthermore, silencing STIM1 expression significantly decreased cytokine production and/or release (Figures 6E,F) with IL-2 (Figure 6F) exhibiting a greater reduction as compared to TNF- α (Figure 6E). These data conclusively demonstrate that SOCE via STIM1 regulates mast cell response following MRGPRX2 activation.



SKF Administration Attenuates Mast Cell-Dependent Inflammation *in vivo*

We next determined if SOCE inhibition affected MRGPRX2-induced responses *in vivo*. Mice express an orthologous receptor to the human MRGPRX2, termed *MrgprB2* (3). The mouse receptor is very similar to MRGPRX2; it is activated by the same ligands, facilitates pseudo-allergic phenotypes, and exhibits high sequence homology. We adopted a previously described model of compound 48/80-induced paw edema that is dependent on *MrgprB2* expression on mouse mast cells (3). Control vehicle (PBS)- or SKF-treated mice were injected with PBS or compound 48/80 in their right and left paws, respectively, and vascular permeability (an indicator of mast cell degranulation) was assessed following i.v. injection of the Evan blue dye. Paw swelling and histamine levels (an indicator of mast cell degranulation) in the serum were also evaluated in these mice. We observed increased dye extravasation (indicative of vascular leakage), paw swelling and serum histamine levels in the mice treated with compound 48/80, as compared to control PBS treated mice (Figures 7A–D). These responses, however, were significantly reduced in the SKF-treated cohort, suggesting that SOCE inhibition by SKF alleviated compound 48/80-induced paw edema.

Additionally, we investigated the role of SOCE in a more prolonged and severe skin inflammation model of pseudo-allergic rosacea. Since LL-37 is elevated in the skin tissues of human patients with rosacea, it has been used for inducing the pathogenesis of experimental rosacea in rodents (17, 58). Specifically, Muto et al. (6) showed that the LL-37 injections in the skin caused rosacea like symptoms in mice that are dependent on the presence of mast cells. LL-37-induced Ca^{2+} mobilization and degranulation were attenuated by SKF in human mast cells *in vitro* (Figures 3C,G). To determine whether SKF also inhibits mouse mast cell response *in vivo*, we pretreated mice with PBS (vehicle) or SKF, followed by multiple LL-37

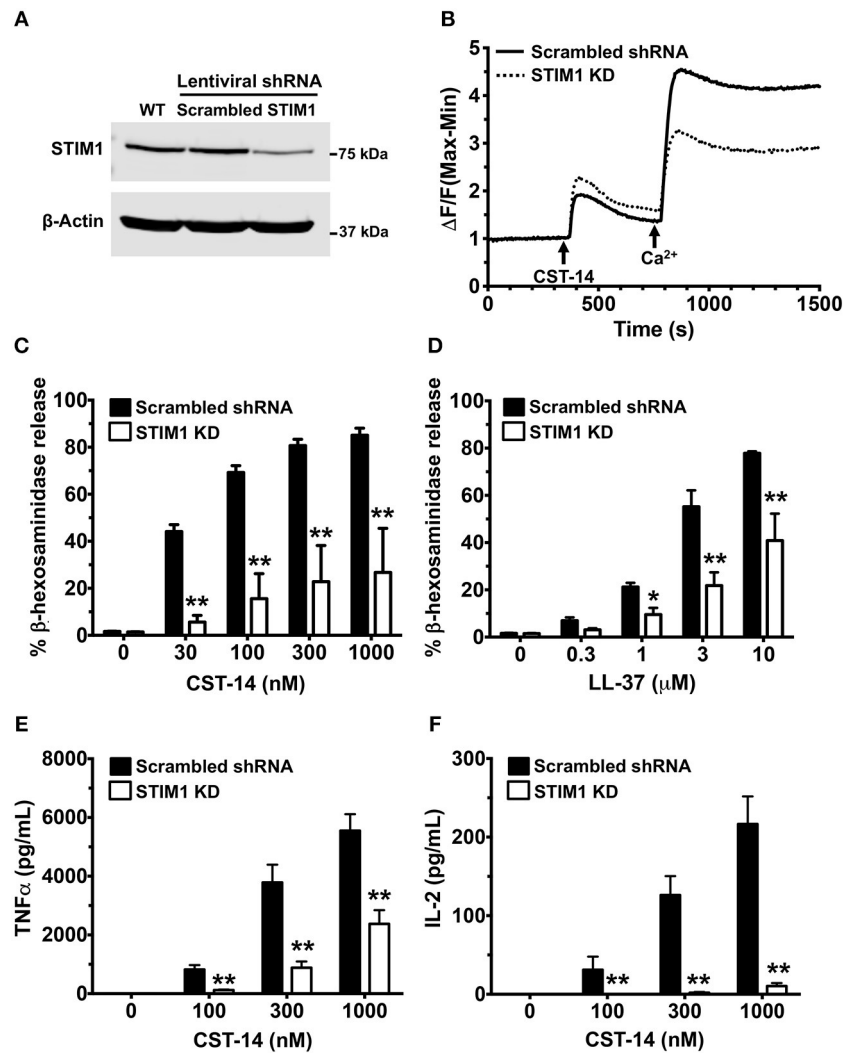
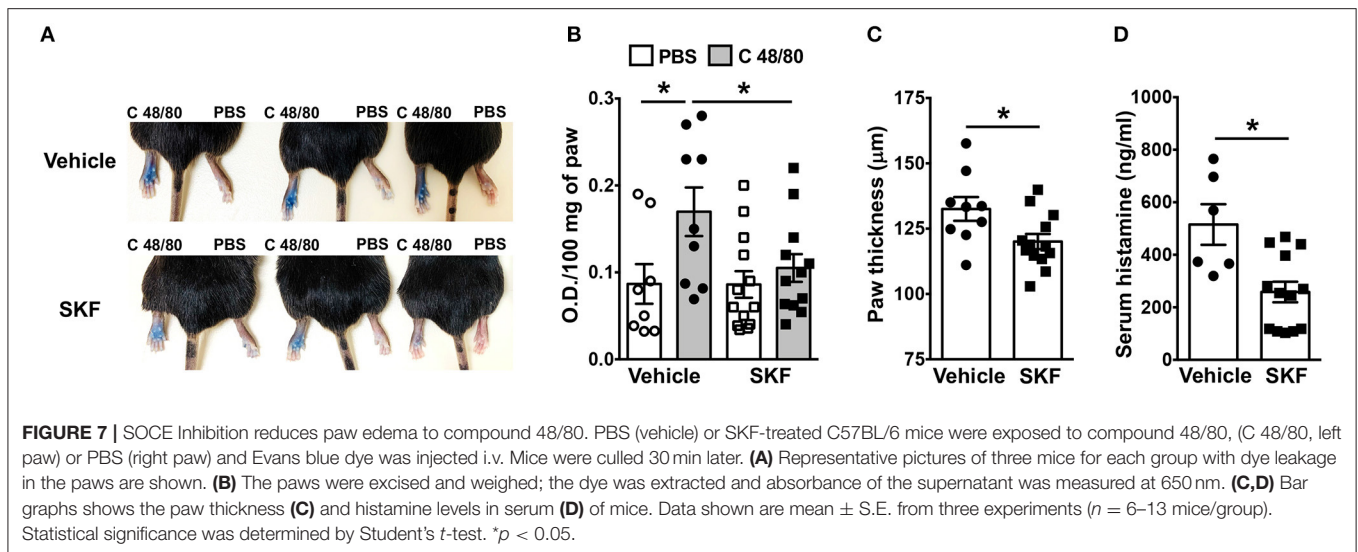


FIGURE 6 | Silencing STIM1 expression inhibits Ca²⁺ mobilization, degranulation and cytokine production in LAD2 mast cells. LAD2 cells were stably transduced with lentivirus containing STIM1 or scrambled shRNA (control). **(A)** A representative blot of STIM1 levels in wild type (WT), scrambled and STIM1 shRNA-transduced cells is shown. **(B)** Control and STIM1 knockdown (KD) cells were labeled with the Calcium 6 dye in Ca²⁺-free buffer. Traces represent the changes in fluorescence following the addition of CST-14 (300 nM) and 2 mM Ca²⁺. **(C,D)** Cells were stimulated with indicated concentrations of CST-14 or LL-37 and β-hexosaminidase release was determined. **(E,F)** Cells were treated with CST-14 for 6 h, and ELISA was performed to estimate TNF-α and IL-2 levels in the supernatants. Data is mean ± S.E. from three experiments. Statistical significance was determined by two-way ANOVA. **p* < 0.05 and ***p* < 0.01.

administrations in the dorsal skin. After 72 h, inflammation was evident in the LL-37 treated mice, although, the SKF treated group showed greatly reduced skin reddening and inflammation (**Figure 8A**). Histological analysis of the skin tissues showed less cellular infiltration and bleeding in the skin of SKF treated mice (**Figure 8B**) resulting in a significant reduction in inflammation score (**Figure 8C**) and epidermal thickness (**Figure 8D**) as compared to the vehicle-treated group. Moreover, RNA analysis of inflammatory markers was consistent with the observed reduction in skin inflammation in the SKF-treated cohort (**Figure 8E**). Specifically, RNA levels of CCL2, IL-6, TNFα, and MMP9 were significantly decreased in the presence of SKF. Importantly, a significant inhibition in RNA

levels of mast cell-associated tryptase (*Tpsab1*) and chymase (*Cmal*) was also observed in the skin of SKF-treated mice. To further examine the role of SKF in attenuating mast cell response *in vivo*, we treated mice with PBS (vehicle) or SKF and exposed them to a single dose of LL-37 in the hind skin. We culled the mice after 30 min of the LL-37 injection and enumerated the numbers of degranulated and non-degranulated mast cells in the skin tissue. Degranulated mast cells exhibited reduced toluidine blue staining intensity and/or dispersed cytoplasmic granules whereas non-degranulated cells were intensely stained and the cytoplasmic granules were not distinctly visible. While there was no difference in the total numbers of mast cells between the PBS and the SKF-treated cohorts of mice (data not shown),



the percentage of degranulated mast cells was significantly reduced in the SKF-treated mice as compared to the control vehicle-treated group (**Figures 8F,G**). Collectively, these data demonstrate that SOCE abrogation by SKF attenuates mast cell-induced inflammation associated with pseudo-allergic reactions *in vivo*.

DISCUSSION

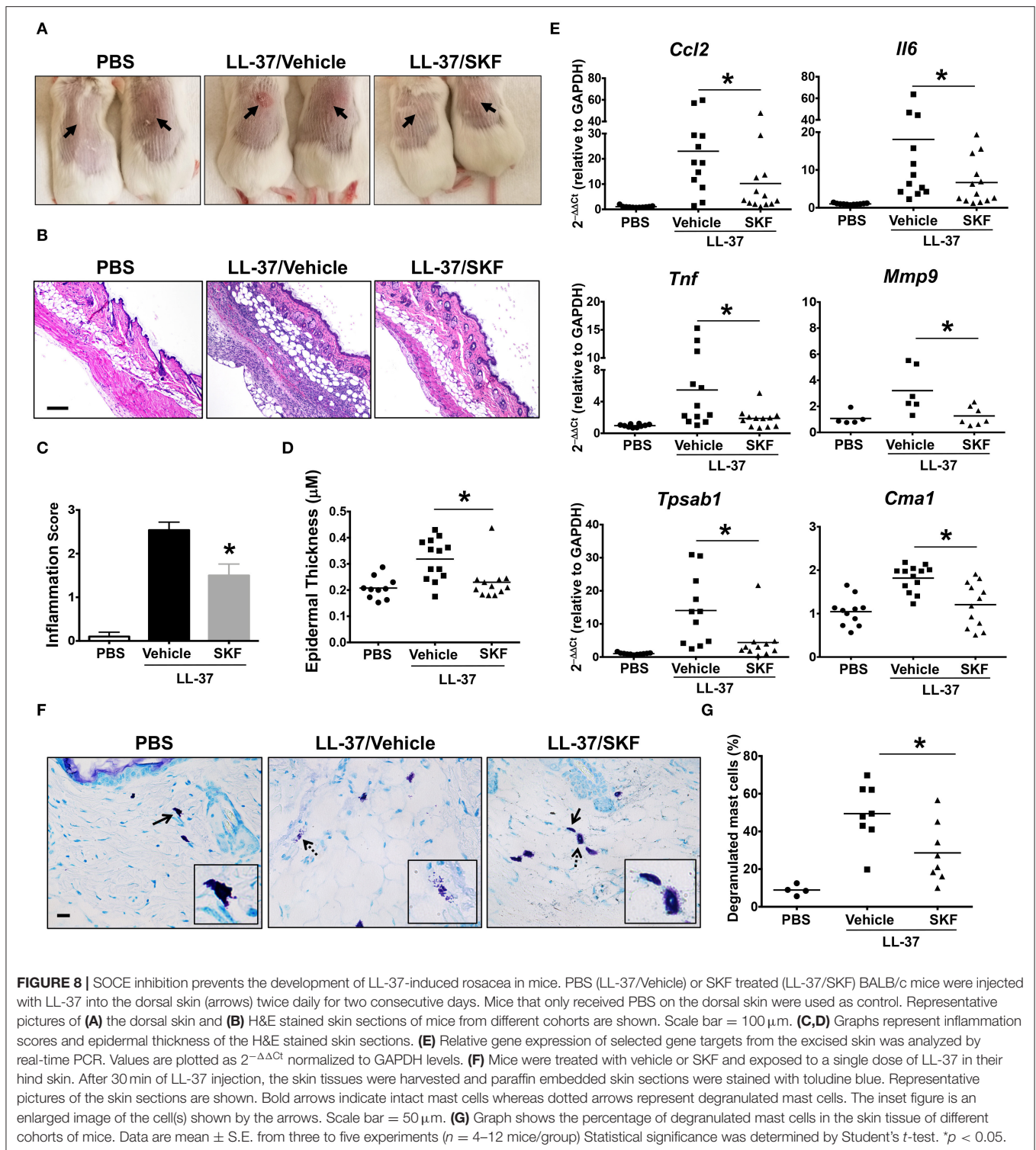
Ca²⁺ signaling in mast cells remains an important facet of proinflammatory cellular activation. As has been shown for the high-affinity IgE receptor FcεRI (29), STIM1 and SOCE are imperative for the proper Ca²⁺ potentiation and mast cell function. In the current study we examined the role of SOCE as a regulator of MRGPRX2/MrgprB2 mediated responses in mast cells. Our *in vitro* and *in vivo* experiments show that SOCE via STIM1 is an important mechanism for potentiating MRGPRX2/MrgprB2 mediated mast cell activation. This observation is consistent with other receptors implicated in immune activation. Fcε (59), Fcγ (60), as well as T (61), and B cells receptors (62), all appear to utilize SOCE mechanisms when activating their respective cell types.

While analyzing the mechanisms of MRGPRX2-mediated Ca²⁺ mobilization in human mast cells, we observed some residual signaling in both SKF-treated cells and STIM1 knockdown cells. While some of this Ca²⁺ influx may be due to inefficiencies of the SKF drug and the incomplete knockdown of STIM1, respectively, it is important to note that the TRPV4 Ca²⁺ channel has been shown to contribute to MRGPRX2 responses and is subject to upregulation when the cells are stimulated (63, 64). It is therefore possible that some residual Ca²⁺ influx occurs via the TRPV4 channels in the presence of SKF. Activation of TRPV4 channels may be

mediated by mechanisms independent of SOCE; however, STIM1 is known to complex with other TRP channels, such as the TRPC subtype and mediate SOCE (65). There may be some degree of activation of TRPV4 by STIM1, although these pathways are yet to be determined. The differential mechanisms utilized by STIM1 and TRPV4 channels to mediate MRGPRX2-induced Ca²⁺ influx and mast cell activation will be the subject of our future investigation.

Mast cell degranulation is promptly initiated by increases of cytosolic Ca²⁺ levels through Ca²⁺-mediated exocytosis. Consistent with our Ca²⁺ mobilization data, SOCE inhibition abrogated most of the degranulation response. Residual degranulation may have been enacted through Ca²⁺-independent signaling pathways or by drawing upon smooth endoplasmic reticulum Ca²⁺ stores. Intracellular signaling events activated by MRGPRX2 are not particularly well-characterized, although, MAP kinase pathways have been shown to be activated in previous studies (56, 66). Our results demonstrated the phosphorylation of ERK1/2 during LL-37 stimulation was significantly reduced in the presence of SKF (**Figure 4**). An interesting finding of the current study was that activation of Akt was not significantly altered by SKF treatment suggesting that SOCE does not contribute to MRGPRX2-induced Akt activation. MAP kinase and Akt pathways are differentially regulated for different receptors (67) and hence it is possible that while SOCE regulates the MAP kinase pathway for MRGPRX2, a SOCE-independent pathway possibly modulates Akt activation.

In agreement with decreased ERK1/2 activation following SOCE inhibition, LAD2 cells exhibited decreased levels of cytokine production in both SKF-treated and STIM1-silenced cells following MRGPRX2 stimulation indicating that the SOCE-ERK1/2 pathway regulates MRGPRX2 cytokine responses in mast cells. However, it is unclear whether the production of cytokines is being reduced or their release from the cell is affected. Given that Ca²⁺ is important in facilitating a variety



of mast cell responses, combined with the decreased ERK1/2 activation in SKF-treated cells, it is conceivable that both the generation as well as the release of cytokines are impaired. LAD2 cells produce copious amounts of pro-inflammatory cytokines such as TNF- α and IL-2 following activation via MRGPRX2. While TNF- α is partially stored in mast cell granules (68),

IL-2 is synthesized *de novo* (69). As levels of both of these cytokines are reduced, the notion that both the production and release of cytokines are decreased by abrogating SOCE is strengthened.

Lastly, we demonstrated that paw edema and experimental rosacea were reduced by SKF administration. These models

induce pseudo-allergic reactions to MrgprB2 agonists, and this response is mast cell-dependent (3, 6). Because of its short duration and acute nature, the paw edema model corresponds with the immediate phase of mast cell response i.e., degranulation. The accumulation of fluids in the paw tissue is due to histamine released by mast cells following degranulation, which causes subsequent vasodilation and vascular leakage. SKF administration prevented histamine secretion and tissue edema through SOCE inhibition in mast cells, thus complementing our *in vitro* degranulation data. Furthermore, hindering the development of rosacea through SKF injection demonstrates the importance of SOCE in the pseudo-allergic pathology. Although other immune cells may participate in exacerbation of inflammation associated with rosacea, mast cells play a critical role in initiating this disease. We have shown that SFK treatment reduced mast cell Ca^{2+} mobilization and degranulation to LL-37 *in vitro* (Figure 3). Accordingly, the pathology of rosacea was reduced by SOCE inhibition *in vivo*; skin histology showed less inflammatory characteristics, and tissue cytokine/chemokine levels were decreased. Importantly, tryptase, and chymase, two important proteases that are stored and secreted by skin mast cells (70), were reduced in SKF-treated mice. Furthermore, the percentage of degranulated mast cells was also reduced in the skin of mice treated with SKF. These data suggested that mast cell activation was debilitated by SOCE inhibition, and therefore, rosacea pathogenesis was reduced. It also possible that in conjunction with abrogating mast cell response, SKF also affects the inflammatory response of other immune cells involved in rosacea pathology such as T cells. Future studies using mice with mast cell- or T cell-specific STIM1 deletion will determine the contribution of STIM1 expression in these cell types in regulating the rosacea response *in vivo*.

Mast cell MRGPRX2 plays a pivotal role in mediating pseudo-allergic reactions to several FDA approved drugs (3, 19–24) and chronic inflammation associated with asthma (18), urticaria (7), and rosacea (6). We have identified a role for SOCE via STIM1 in regulating MRGPRX2 responses in mast cells. Considering three phases of the mast cell response- immediate Ca^{2+} mobilization, acute degranulation, and latent cytokine production; SOCE inhibition attenuated each of the three steps and reduced inflammation in MRGPRX2 dependent allergic models. Given that SOCE via STIM1 promotes responses of FcεRI (29) and MRGPRX2, two important mast cells receptors that mediate allergy in humans; future studies designed to characterize this mechanism further may lead to the development of novel therapeutic approaches for the treatment of allergic diseases.

REFERENCES

1. Metcalfe DD, Baram D, Mekori YA. Mast cells. *Physiol Rev.* (1997) 77:1033–79. doi: 10.1152/physrev.1997.77.4.1033
2. von Bubnoff D, Novak N, Kraft S, Bieber T. The central role of FcεRI in allergy. *Clin Exp Dermatol.* (2003) 28:184–7. doi: 10.1046/j.1365-2230.2003.01209.x

DATA AVAILABILITY STATEMENT

All datasets generated for this study are included in the article/**Supplementary Material**.

ETHICS STATEMENT

The animal studies were reviewed and approved by Michigan State University's IACUC and Animal Care Program. Studies with human samples were approved by the Internal Review Board (IRB) of the University of South Carolina.

AUTHOR CONTRIBUTIONS

CO and AK performed experiments, interpreted data, and wrote parts of the manuscript. CY, RN, MG, and GG performed experiments and analyzed the data. HS conceived the study, planned the experiments, and wrote the manuscript.

FUNDING

This work was supported by a grant from the National Institutes of Health, National Heart Lung and Blood Institute (5R00HL121073) (HS) and Michigan State University's startup funds (HS). CO was supported by an Undergraduate Research Scholarship from Michigan State University. RN was an NHLBI scholar, and his research training was supported through an NIH award, 5-R25-HL108864 to Elahé Crockett, Ph.D., MS, Director of REPID (Research Education to Increase Diversity in Health Researchers) program at Michigan State University.

ACKNOWLEDGMENTS

We thank Drs. Arnold Kirshenbaum and Dean Metcalfe at The Laboratory of Allergic Disease at the National Institutes of Health (Bethesda, MD) for providing us the LAD2 mast cells. We also thank the histology and mass spectrometry and metabolomics core facilities at Michigan State University for mouse skin tissue histology, H&E staining, and LC-MS/MS analysis of serum samples. We also thank Dr. Rupali Das, Brianna Callahan, and Tanwir Hashem for critical review of the manuscript and helpful discussions regarding the project.

SUPPLEMENTARY MATERIAL

The Supplementary Material for this article can be found online at: <https://www.frontiersin.org/articles/10.3389/fimmu.2019.03143/full#supplementary-material>

3. McNeil BD, Pundir P, Meeker S, Han L, Undem BJ, Kulka M, et al. Identification of a mast-cell-specific receptor crucial for pseudo-allergic drug reactions. *Nature.* (2015) 519:237–41. doi: 10.1038/nature14022
4. Subramanian H, Gupta K, Ali H. Roles of Mas-related G protein-coupled receptor X2 on mast cell-mediated host defense, pseudoallergic drug reactions, and chronic inflammatory diseases. *J Allergy Clin Immunol.* (2016) 138:700–10. doi: 10.1016/j.jaci.2016.04.051

5. Ali H. Emerging roles for MAS-related G protein-coupled receptor-X2 in host defense peptide, opioid, and neuropeptide-mediated inflammatory reactions. *Adv Immunol.* (2017) 136:123–62. doi: 10.1016/bs.ai.2017.06.002
6. Muto Y, Wang Z, Vanderberghe M, Two A, Gallo RL, Di Nardo A. Mast cells are key mediators of cathelicidin-initiated skin inflammation in rosacea. *J Invest Dermatol.* (2014) 134:2728–36. doi: 10.1038/jid.2014.222
7. Fujisawa D, Kashiwakura J, Kita H, Kikukawa Y, Fujitani Y, Sasaki-Sakamoto T, et al. Expression of Mas-related gene X2 on mast cells is upregulated in the skin of patients with severe chronic urticaria. *J Allergy Clin Immunol.* (2014) 134:622–33.e629. doi: 10.1016/j.jaci.2014.05.004
8. Azimi E, Reddy VB, Lerner EA. Brief communication: MRGPRX2, atopic dermatitis and red man syndrome. *Itch.* (2017) 2:5. doi: 10.1097/itx.0000000000000005
9. Okamura Y, Mishima S, Kashiwakura JI, Sasaki-Sakamoto T, Toyoshima S, Kuroda K, et al. The dual regulation of substance P-mediated inflammation via human synovial mast cells in rheumatoid arthritis. *Allergol Int.* (2017) 66S:S9–20. doi: 10.1016/j.alit.2017.03.002
10. Robas N, Mead E, Fidock M. MrgX2 is a high potency cortistatin receptor expressed in dorsal root ganglion. *J Biol Chem.* (2003) 278:44400–4. doi: 10.1074/jbc.M302456200
11. Subramanian H, Kashem SW, Collington SJ, Qu H, Lambris JD, Ali H. PMX-53 as a dual CD88 antagonist and an agonist for Mas-related gene 2 (MrgX2) in human mast cells. *Mol Pharmacol.* (2011) 79:1005–13. doi: 10.1124/mol.111.071472
12. Subramanian H, Gupta K, Lee D, Bayir AK, Ahn H, Ali H. beta-Defensins activate human mast cells via Mas-related gene X2. *J Immunol.* (2013) 191:345–52. doi: 10.4049/jimmunol.1300023
13. Subramanian H, Gupta K, Guo Q, Price R, Ali H. Mas-related gene X2 (MrgX2) is a novel G protein-coupled receptor for the antimicrobial peptide LL-37 in human mast cells: resistance to receptor phosphorylation, desensitization, and internalization. *J Biol Chem.* (2011) 286:44739–49. doi: 10.1074/jbc.M111.277152
14. Yu Y, Zhang Y, Zhang Y, Lai Y, Chen W, Xiao Z, et al. LL-37-induced human mast cell activation through G protein-coupled receptor MrgX2. *Int Immunopharmacol.* (2017) 49:6–12. doi: 10.1016/j.intimp.2017.05.016
15. Tatemoto K, Nozaki Y, Tsuda R, Konno S, Tomura K, Furuno M, et al. Immunoglobulin E-independent activation of mast cell is mediated by Mrg receptors. *Biochem Biophys Res Commun.* (2006) 349:1322–8. doi: 10.1016/j.bbrc.2006.08.177
16. Kashem SW, Subramanian H, Collington SJ, Magotti P, Lambris JD, Ali H. G protein coupled receptor specificity for C3a and compound 48/80-induced degranulation in human mast cells: roles of Mas-related genes MrgX1 and MrgX2. *Eur J Pharmacol.* (2011) 668:299–304. doi: 10.1016/j.ejphar.2011.06.027
17. Reinholz M, Ruzicka T, Schaubert J. Cathelicidin LL-37: an antimicrobial peptide with a role in inflammatory skin disease. *Ann Dermatol.* (2012) 24:126–35. doi: 10.5021/ad.2012.24.2.126
18. Manorak W, Idahosa C, Gupta K, Roy S, Panettieri R Jr, Ali H. Upregulation of Mas-related G Protein coupled receptor X2 in asthmatic lung mast cells and its activation by the novel neuropeptide hemokinin-1. *Respir Res.* (2018) 19:1. doi: 10.1186/s12931-017-0698-3
19. Che D, Rui L, Cao J, Wang J, Zhang Y, Ding Y, et al. Cisatracurium induces mast cell activation and pseudo-allergic reactions via MRGPRX2. *Int Immunopharmacol.* (2018) 62:244–50. doi: 10.1016/j.intimp.2018.07.020
20. Che D, Wang J, Ding Y, Liu R, Cao J, Zhang Y, et al. Mivacurium induce mast cell activation and pseudo-allergic reactions via MAS-related G protein coupled receptor-X2. *Cell Immunol.* (2018) 332:121–8. doi: 10.1016/j.cellimm.2018.08.005
21. Navines-Ferrer A, Serrano-Candelas E, Lafuente A, Munoz-Cano R, Martin M, Gastaminza G. MRGPRX2-mediated mast cell response to drugs used in perioperative procedures and anaesthesia. *Sci Rep.* (2018) 8:11628. doi: 10.1038/s41598-018-29965-8
22. Zhang T, Che D, Liu R, Han S, Wang N, Zhan Y, et al. Typical antimicrobials induce mast cell degranulation and anaphylactoid reactions via MRGPRX2 and its murine homologue MRGPRB2. *Eur J Immunol.* (2017) 47:1949–58. doi: 10.1002/eji.201746951
23. Liu R, Hu S, Zhang Y, Che D, Cao J, Wang J, et al. Mast cell-mediated hypersensitivity to fluoroquinolone is MRGPRX2 dependent. *Int Immunopharmacol.* (2019) 70:417–27. doi: 10.1016/j.intimp.2019.02.001
24. Porebski G, Kwiecien K, Pawica M, Kwitniewski M. Mas-Related G Protein-Coupled Receptor-X2 (MRGPRX2) in Drug Hypersensitivity Reactions. *Front Immunol.* (2018) 9:3027. doi: 10.3389/fimmu.2018.03027
25. Huber M, Helgason CD, Damen JE, Liu L, Humphries RK, Krystal G. The src homology 2-containing inositol phosphatase (SHIP) is the gatekeeper of mast cell degranulation. *Proc Natl Acad Sci USA.* (1998) 95:11330–5. doi: 10.1073/pnas.95.19.11330
26. Ferguson SS. Evolving concepts in G protein-coupled receptor endocytosis: the role in receptor desensitization and signaling. *Pharmacol Rev.* (2001) 53:1–24. Available online at: <http://pharmrev.aspetjournals.org/content/53/1/1>
27. Shaw PJ, Feske S. Physiological and pathophysiological functions of SOCE in the immune system. *Front Biosci.* (2012) 4:2253–68. doi: 10.2741/e540
28. Bergmeier W, Weidinger C, Zee I, Feske S. Emerging roles of store-operated Ca(2+)(+) entry through STIM and Orai proteins in immunity, hemostasis and cancer. *Channels.* (2013) 7:379–91. doi: 10.4161/chan.24302
29. Baba Y, Nishida K, Fujii Y, Hirano T, Hikida M, Kurosaki T. Essential function for the calcium sensor STIM1 in mast cell activation and anaphylactic responses. *Nat Immunol.* (2008) 9:81–8. doi: 10.1038/ni1546
30. Smyth JT, Hwang SY, Tomita T, DeHaven WI, Mercer JC, Putney JW. Activation and regulation of store-operated calcium entry. *J Cell Mol Med.* (2010) 14:2337–49. doi: 10.1111/j.1582-4934.2010.01168.x
31. Putney JW, Steinckwich-Besancon N, Numaga-Tomita T, Davis FM, Desai PN, D'Agostin DM, et al. The functions of store-operated calcium channels. *Biochim Biophys Acta Mol Cell Res.* (2017) 1864:900–6. doi: 10.1016/j.bbamcr.2016.11.028
32. Chen YC, Chang YC, Chang HA, Lin YS, Tsao CW, Shen MR, et al. Differential Ca(2+) mobilization and mast cell degranulation by FcepsilonRI- and GPCR-mediated signaling. *Cell Calcium.* (2017) 67:31–9. doi: 10.1016/j.ceca.2017.08.002
33. Inoh Y, Haneda A, Tadokoro S, Yokawa S, Furuno T. Cationic liposomes suppress intracellular calcium ion concentration increase via inhibition of PI3 kinase pathway in mast cells. *Biochim Biophys Acta Biomembr.* (2017) 1859:2461–6. doi: 10.1016/j.bbamem.2017.09.025
34. Yang B, Li JJ, Cao JJ, Yang C-B, Liu J, Ji Q-M, et al. Polydatin attenuated food allergy via store-operated calcium channels in mast cell. *World J Gastroenterol.* (2013) 19:3980–9. doi: 10.3748/wjg.v19.i25.3980
35. Ashmole I, Duffy SM, Leyland ML, Bradding P. The contribution of Orai(CRACM)1 and Orai(CRACM)2 channels in store-operated Ca2+ entry and mediator release in human lung mast cells. *PLoS ONE.* (2013) 8:e74895. doi: 10.1371/journal.pone.0074895
36. Kirshenbaum AS, Akin C, Wu Y, Rottem M, Goff JP, Beaven MA, et al. Characterization of novel stem cell factor responsive human mast cell lines LAD 1 and 2 established from a patient with mast cell sarcoma/leukemia; activation following aggregation of FcepsilonRI or FcgammaRI. *Leuk Res.* (2003) 27:677–82. doi: 10.1016/S0145-2126(02)0343-0
37. Troupin A, Shirley D, Londono-Renteria B, Watson AM, McHale C, Hall A, et al. A role for human skin mast cells in dengue virus infection and systemic spread. *J Immunol.* (2016) 197:4382–91. doi: 10.4049/jimmunol.1600846
38. McHale C, Mohammed Z, Gomez G. Human skin-derived mast cells spontaneously secrete several angiogenesis-related factors. *Front Immunol.* (2019) 10:1445. doi: 10.3389/fimmu.2019.01445
39. McHale C, Mohammed Z, Deppen J, Gomez G. Interleukin-6 potentiates FcepsilonRI-induced PGD2 biosynthesis and induces VEGF from human *in situ*-matured skin mast cells. *Biochim Biophys Acta Gen Subj.* (2018) 1862:1069–78. doi: 10.1016/j.bbagen.2018.01.020
40. Guo Y, Mochizuki T, Morii E, Kitamura Y, Maeyama K. Role of mast cell histamine in the formation of rat paw edema: a microdialysis study. *Eur J Pharmacol.* (1997) 331:237–43. doi: 10.1016/S0014-2999(97)01002-9
41. Chimalakonda KC, Pang E, Weaver JL, Howard KE, Patel V, Boyne MT, 2nd. Development and validation of a liquid-chromatography tandem mass spectrometry method to determine *in vitro* and *in vivo* histamine release. *J Pharm Biomed Anal.* (2015) 102:494–9. doi: 10.1016/j.jpba.2014.10.016

42. Schwartz J, Moreno E, Calvo A, et al. Combination of paromomycin plus human anti-TNF- α antibodies to control the local inflammatory response in BALB/ mice with cutaneous leishmaniasis lesions. *J Dermatol Sci.* (2018) 92:78–88. doi: 10.1016/j.jdermsci.2018.07.005
43. Ngo Nyekel F, Pacreau E, Benadda S, Msallam R, Åbrink M, Pejler G, et al. Mast cell degranulation exacerbates skin rejection by enhancing neutrophil recruitment. *Front Immunol.* (2018) 9:2690. doi: 10.3389/fimmu.2018.02690
44. Prakriya M. The molecular physiology of CRAC channels. *Immunol Rev.* (2009) 231:88–98. doi: 10.1111/j.1600-065X.2009.00820.x
45. Prakriya M, Feske S, Gwack Y, Srikanth S, Rao A, Hogan PG. Orai1 is an essential pore subunit of the CRAC channel. *Nature.* (2006) 443:230–3. doi: 10.1038/nature05122
46. Chen KH, Liu H, Yang L, Jin MW, Li GR. SKF-96365 strongly inhibits voltage-gated sodium current in rat ventricular myocytes. *Pflugers Arch.* (2015) 467:1227–36. doi: 10.1007/s00424-014-1565-4
47. Singh A, Hildebrand ME, Garcia E, Snutch TP. The transient receptor potential channel antagonist SKF96365 is a potent blocker of low-voltage-activated T-type calcium channels. *Br J Pharmacol.* (2010) 160:1464–75. doi: 10.1111/j.1476-5381.2010.00786.x
48. Lansu K, Karpiak J, Liu J, Huang XP, McCorvy JD, Kroeze WK, et al. *In silico* design of novel probes for the atypical opioid receptor MRGPRX2. *Nat Chem Biol.* (2017) 13:529–36. doi: 10.1038/nchembio.2334
49. Maeyama K, Hohman RJ, Metzger H, Beaven MA. Quantitative relationships between aggregation of IgE receptors, generation of intracellular signals, and histamine secretion in rat basophilic leukemia (2H3) cells. Enhanced responses with heavy water. *J Biol Chem.* (1986) 261:2583–92.
50. Kulczycki A Jr., Isersky C, Metzger H. The interaction of IgE with rat basophilic leukemia cells. I. Evidence for specific binding of IgE. *J Exp Med.* (1974) 139:600–16. doi: 10.1084/jem.139.3.600
51. Kulczycki A Jr., Metzger H. The interaction of IgE with rat basophilic leukemia cells. II. Quantitative aspects of the binding reaction. *J Exp Med.* (1974) 140:1676–95. doi: 10.1084/jem.140.6.1676
52. Robertson D, Holowka D, Baird B. Cross-linking of immunoglobulin E-receptor complexes induces their interaction with the cytoskeleton of rat basophilic leukemia cells. *J Immunol.* (1986) 136:4565–72.
53. Fewtrell C, Metzger H. Larger oligomers of IgE are more effective than dimers in stimulating rat basophilic leukemia cells. *J Immunol.* (1980) 125:701–10.
54. Passante E, Frankish N. The RBL-2H3 cell line: its provenance and suitability as a model for the mast cell. *Inflamm Res.* (2009) 58:737–45. doi: 10.1007/s00011-009-0074-y
55. Chompunud Na Ayudhya C, Roy S, Alkanfari I, Ganguly A, Ali H. Identification of gain and loss of function missense variants in MRGPRX2's transmembrane and intracellular domains for mast cell activation by substance P. *Int J Mol Sci.* (2019) 20:E5247. doi: 10.3390/ijms20215247
56. Niyonsaba F, Ushio H, Hara M, Yokoi H, Tominaga M, Takamori K, et al. Antimicrobial peptides human beta-defensins and cathelicidin LL-37 induce the secretion of a pruritogenic cytokine IL-31 by human mast cells. *J Immunol.* (2010) 184:3526–34. doi: 10.4049/jimmunol.0900712
57. Kiatsurayanon C, Niyonsaba F, Chieosilapatham P, Okumura K, Ikeda S, Ogawa H. Angiogenic peptide (AG)-30/5C activates human keratinocytes to produce cytokines/chemokines and to migrate and proliferate via MrgX receptors. *J Dermatol Sci.* (2016) 83:190–9. doi: 10.1016/j.jdermsci.2016.05.006
58. Salzer S, Kresse S, Hirai Y, Koglin S, Reinholz M, Ruzicka T, et al. Cathelicidin peptide LL-37 increases UVB-triggered inflammasome activation: possible implications for rosacea. *J Dermatol Sci.* (2014) 76:173–9. doi: 10.1016/j.jdermsci.2014.09.002
59. Wajdner HE, Farrington J, Barnard C, Peachell PT, Schnackenberg CG, Marino JP, Jr, et al. Orai and TRPC channel characterization in Fc ϵ RI-mediated calcium signaling and mediator secretion in human mast cells. *Physiol Rep.* (2017) 5:e13166. doi: 10.14814/phy2.13166
60. Braun A, Gessner JE, Varga-Szabo D, Syed SN, Konrad S, Stegner D, et al. STIM1 is essential for Fc γ receptor activation and autoimmune inflammation. *Blood.* (2009) 113:1097–104. doi: 10.1182/blood-2008-05-158477
61. Lioudyno MI, Kozak JA, Penna A, Safrina O, Zhang SL, Sen D, et al. Orai1 and STIM1 move to the immunological synapse and are up-regulated during T cell activation. *Proc Natl Acad Sci USA.* (2008) 105:2011–6. doi: 10.1073/pnas.0706122105
62. Morita T, Tanimura A, Baba Y, Kurosaki T, Tojyo Y. A Stim1-dependent, noncapacitative Ca $^{2+}$ -entry pathway is activated by B-cell-receptor stimulation and depletion of Ca $^{2+}$. *J Cell Sci.* (2009) 122(Pt 8):1220–8. doi: 10.1242/jcs.041640
63. Mascarenhas NL, Wang Z, Chang YL, Di Nardo A. TRPV4 mediates mast cell activation in cathelicidin-induced rosacea inflammation. *J Invest Dermatol.* (2017) 137:972–5. doi: 10.1016/j.jid.2016.10.046
64. Sulk M, Seeliger S, Aubert J, Schwab VD, Cevikbas F, Rivier M, et al. Distribution and expression of non-neuronal transient receptor potential (TRPV) ion channels in rosacea. *J Invest Dermatol.* (2012) 132:1253–62. doi: 10.1038/jid.2011.424
65. Worley PF, Zeng W, Huang GN, Yuan JP, Kim JY, Lee MG, et al. TRPC channels as STIM1-regulated store-operated channels. *Cell Calcium.* (2007) 42:205–11. doi: 10.1016/j.ceca.2007.03.004
66. Chen X, Niyonsaba F, Ushio H, Nagaoka I, Ikeda S, Okumura K, et al. Human cathelicidin LL-37 increases vascular permeability in the skin via mast cell activation, and phosphorylates MAP kinases p38 and ERK in mast cells. *J Dermatol Sci.* (2006) 43:63–6. doi: 10.1016/j.jdermsci.2006.03.001
67. Mendoza MC, Er EE, Blenis J. The Ras-ERK and PI3K-mTOR pathways: cross-talk and compensation. *Trends Biochem Sci.* (2011) 36:320–8. doi: 10.1016/j.tibs.2011.03.006
68. Olszewski MB, Groot AJ, Dastyk J, Knol EF. TNF trafficking to human mast cell granules: mature chain-dependent endocytosis. *J Immunol.* (2007) 178:5701–9. doi: 10.4049/jimmunol.178.9.5701
69. Grutzkau A, Kruger-Krasagakes S, Baumeister H, Schwarz C, Kögel H, Welker P, et al. Synthesis, storage, and release of vascular endothelial growth factor/vascular permeability factor (VEGF/VPF) by human mast cells: implications for the biological significance of VEGF206. *Mol Biol Cell.* (1998) 9:875–84. doi: 10.1091/mbc.9.4.875
70. Caughey GH. Mast cell proteases as protective and inflammatory mediators. *Adv Exp Med Biol.* (2011) 716:212–34. doi: 10.1007/978-1-4419-9533-9_12

Conflict of Interest: The authors declare that the research was conducted in the absence of any commercial or financial relationships that could be construed as a potential conflict of interest.

Copyright © 2020 Occhiuto, Kammala, Yang, Nellutla, Garcia, Gomez and Subramanian. This is an open-access article distributed under the terms of the Creative Commons Attribution License (CC BY). The use, distribution or reproduction in other forums is permitted, provided the original author(s) and the copyright owner(s) are credited and that the original publication in this journal is cited, in accordance with accepted academic practice. No use, distribution or reproduction is permitted which does not comply with these terms.